Supplementary Material (ESI) for Chemical Communications

Supporting Information

Temperature-dependent Charge Distribution in Three-Dimensional Homochiral Cadmium Camphorates

Jian Zhang, Xianhui Bu*

Department of Chemistry and Biochemistry, California State University, Long Beach, 1250 Bellflower Boulevard, Long Beach, CA 90840 E-mail: xbu@csulb.edu

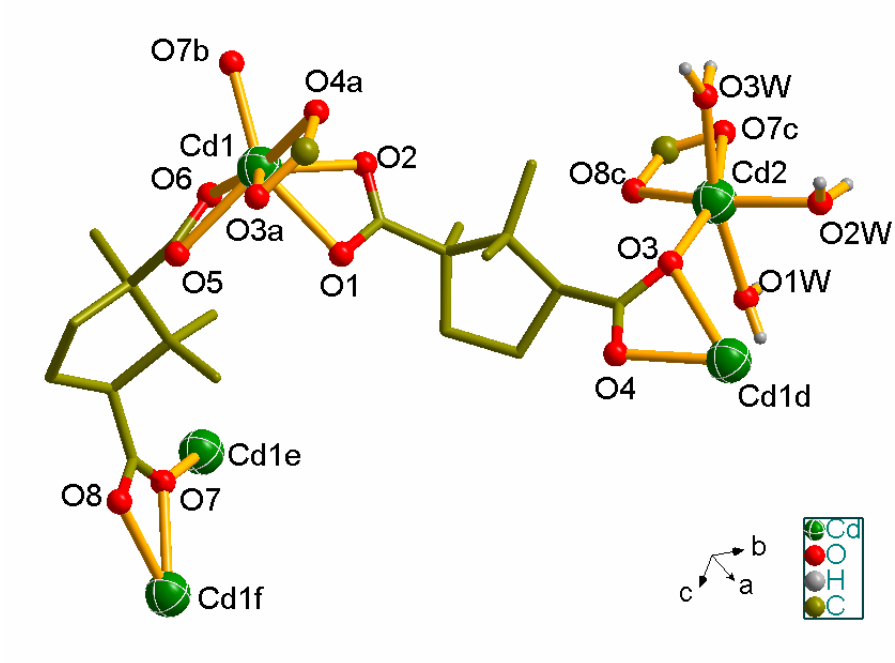

Figure S1. The atomic labeling scheme showing the local coordination environments of cadmium cations in **1**. Atoms with labels containing "a-f" are generated by symmetry operations (Symmetry codes: a = -0.5+x, -0.5-y, 0.25-z; b = -0.5+x, -1.5-y, 0.25-z; c = -0.5-y, -0.5+x, 0.25+z; d = 0.5+x, -0.5-y, 0.25-z; e = 0.5+x, -1.5-y, 0.25-z; f = 0.5+y, -0.5-x, 0.25+z)

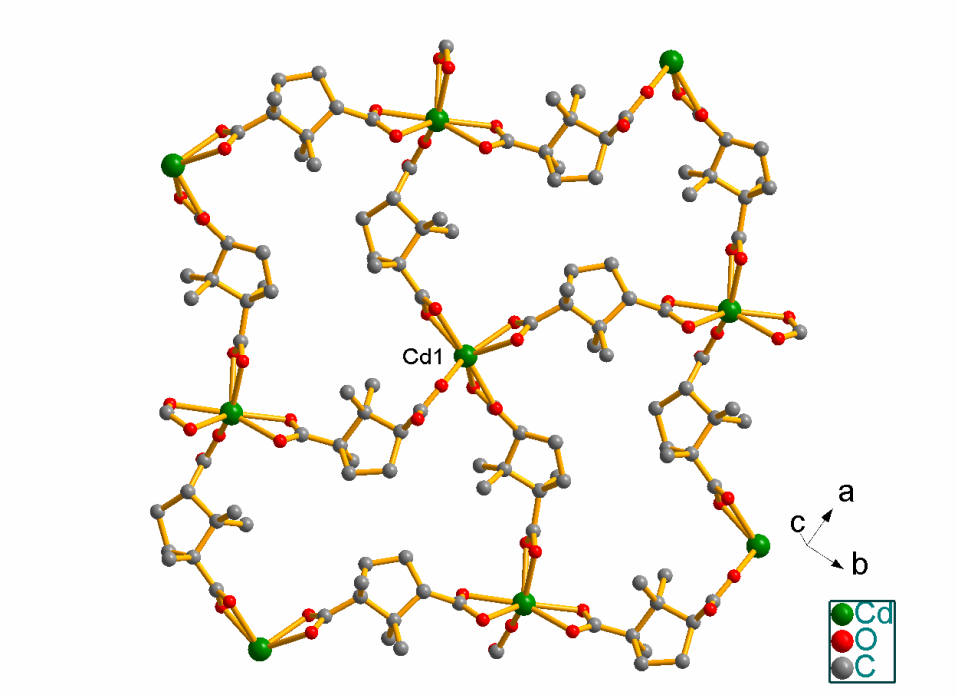

Figure S2. The 2D layer formed by D-Cam ligands bridging Cd1 atoms in **1**.

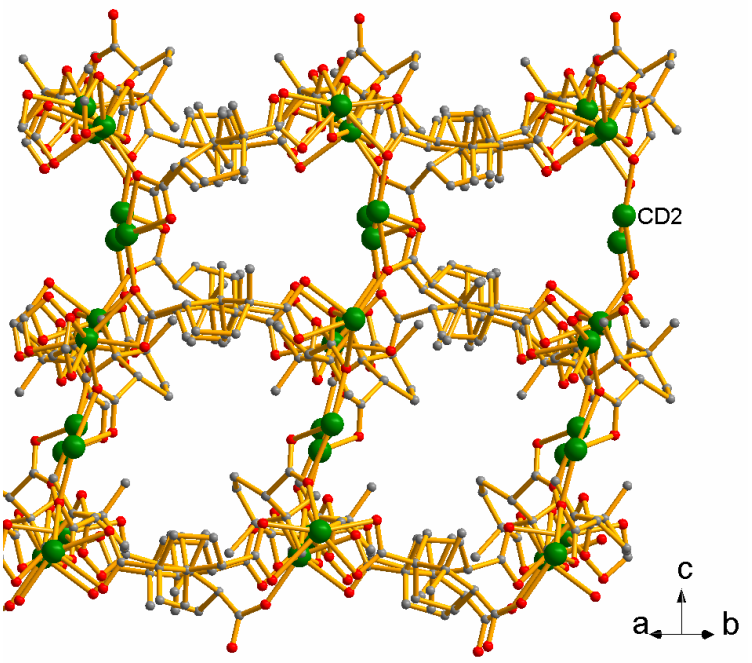

Figure S3. The 3D packing structure of **1**, showing 2D layers connected by Cd2 atoms. It exhibits 6-connected pcu net by connecting all the Cd2+ sites where the Cd1 centers behave as 6-connected nodes and the Cd2 centers behave as 2-connected nodes.

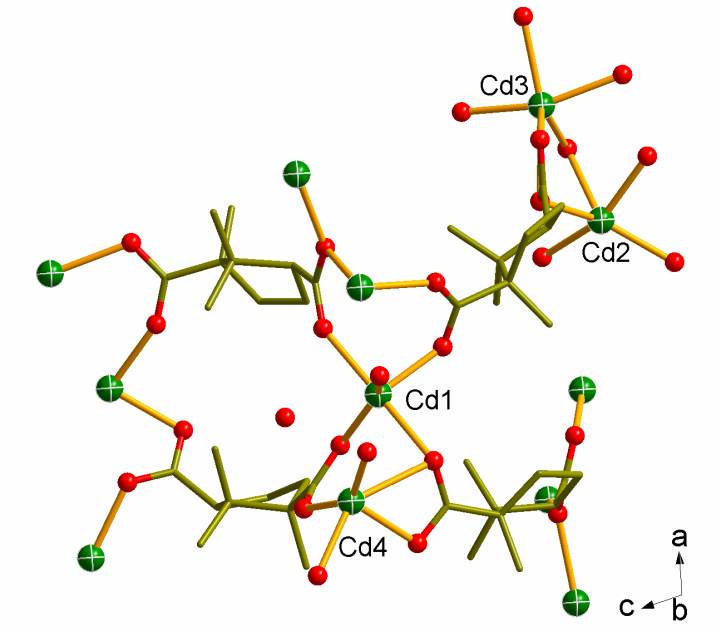

Figure S4. A fragment of the 3-D framework in **2** showing the local bonding environments of cadmium cations.

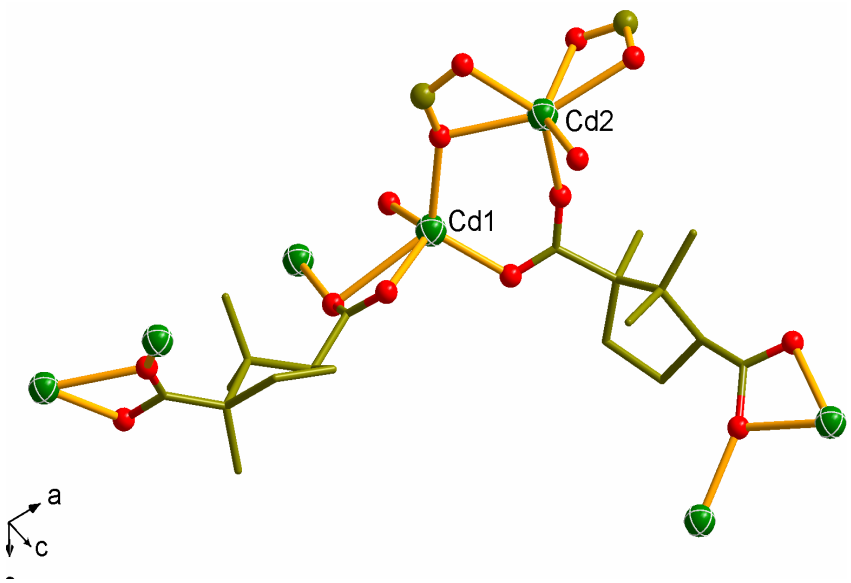

Figure S5. A fragment of the 3-D framework in **3** showing the local bonding environments of cadmium cations.

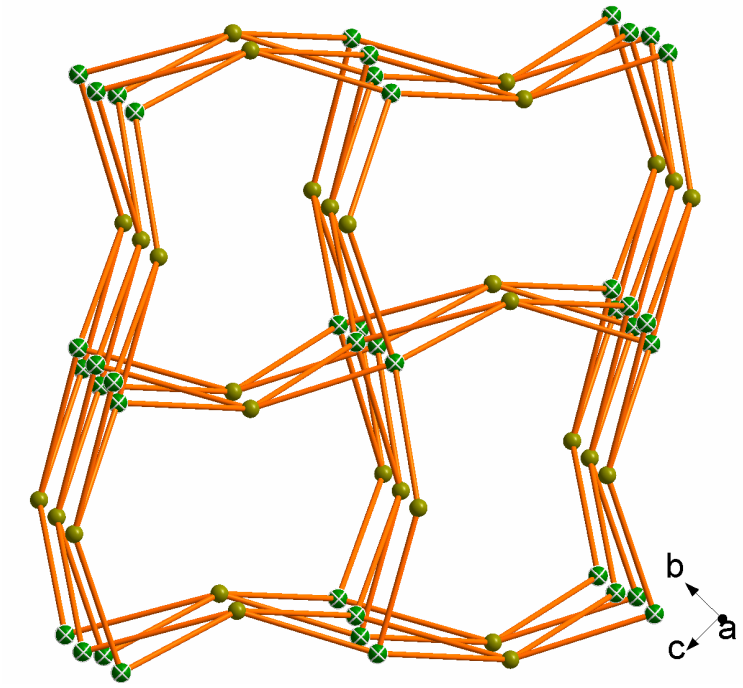

Figure S6. View of the distorted PtS topological net of **3**. The D-Cam ligands are reduced as planar 4-connected nodes (dark yellow) and the Cd atoms are reduced as tetrahedral nodes (green).

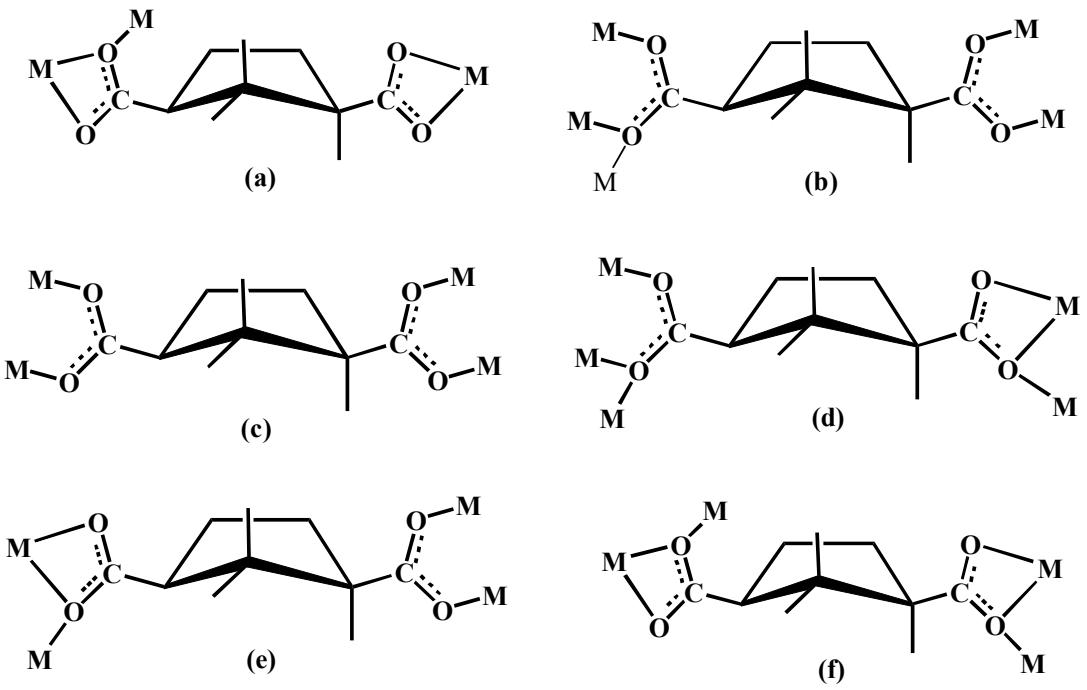

Scheme S1. Six coordination modes of the D-Cam ligands observed in 1 (a), 2 (b-e), and 3 (e, f).

Table S1. The characteristic bands of the carboxylate groups in the IR spectrum of the compounds

Compound	υ_{asym} (cm^{-1})	υ_{sym} (cm^{-1})
1	1583	1403
2	1600, 1539	1417, 1368
3	1615, 1537	1403, 1366

υ_{asym} = asymmetric vibration; υ_{sym} = symmetric vibration

Thermal Analysis The simultaneous DSC-TGA thermal analysis was performed on TA Instruments SDT Q600 under the flowing nitrogen atmosphere. The flow rate of the nitrogen gas was controlled at about 100 mL per minute.

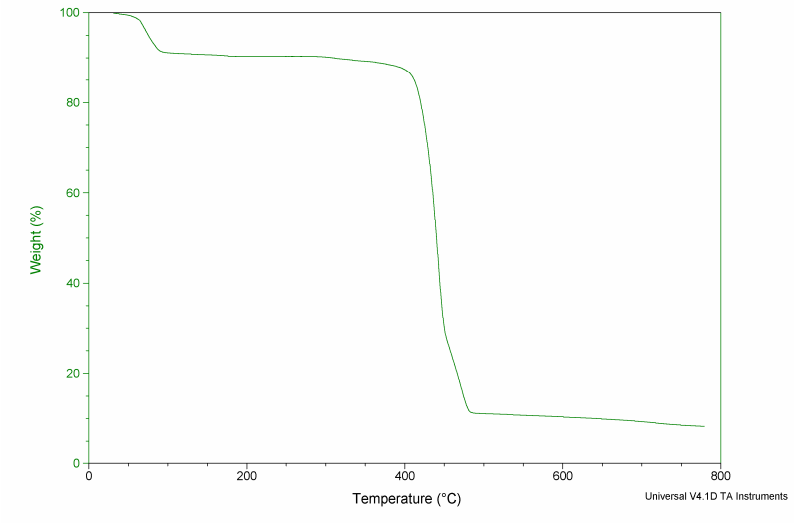

Figure S7. The TGA diagram of **1**.

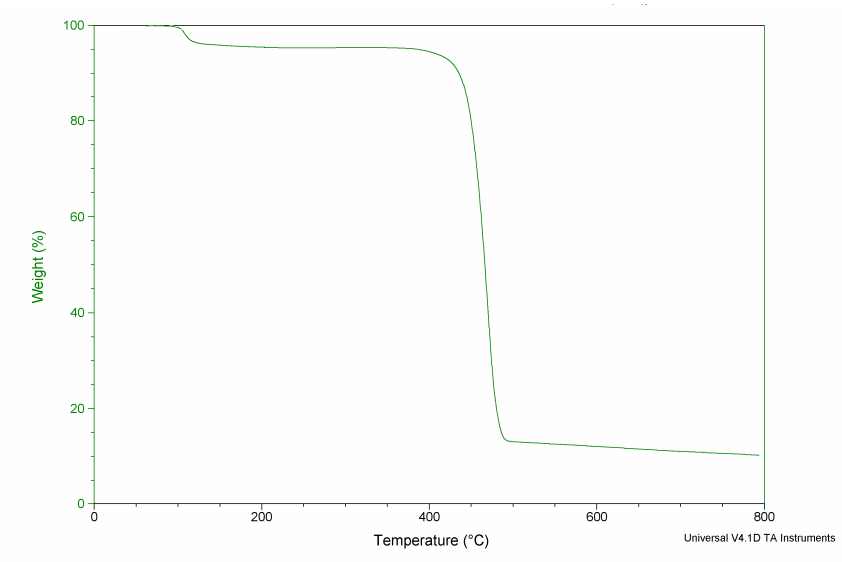

Figure S8. The TGA diagram of **2**.

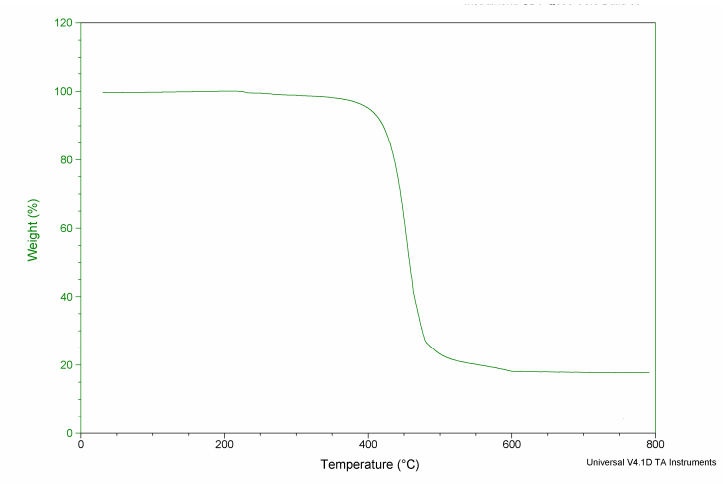

Figure S9. The TGA diagram of **3**.

X-ray Powder Diffraction X-ray powder diffraction experiments were performed on a Bruker D8 Advance X-ray powder diffractometer operating at 40kV and 40mA (CuKα radiation, λ = 1.5418Å). The data collection was carried out with a step size of 0.03 degree and counting time of 1s per step. The 2-theta angular range is from 5 to 40 degrees.

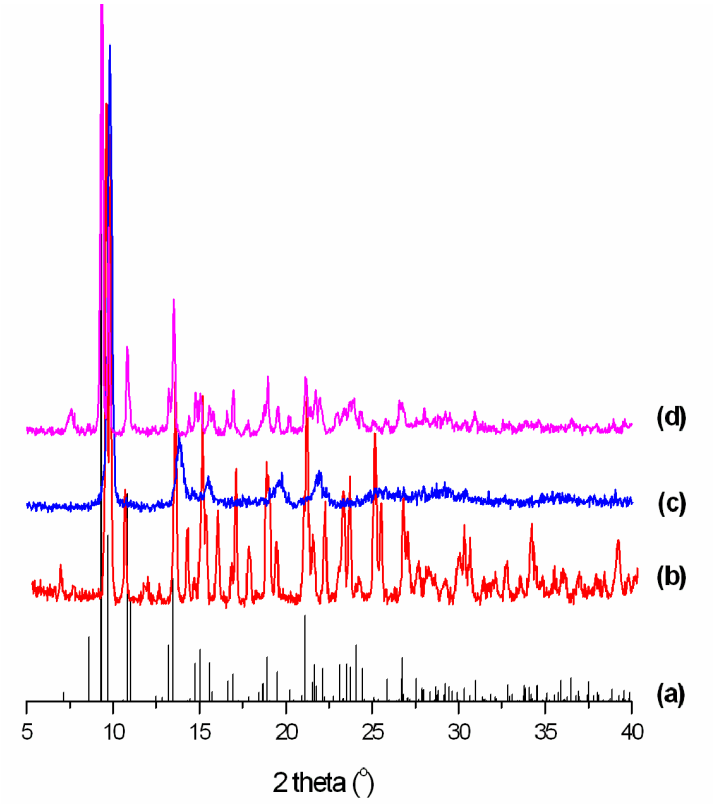

Figure S10. XPRD patterns for **1**: (a) calculated on the basis of the structure determined by single-crystal X-ray diffraction; (b) taken at room temperature; (c) dehydrated at 120 ^{o}C; (d) rehydrated in mixed water/ethanol (1:3 ratio) solution at room temperature.

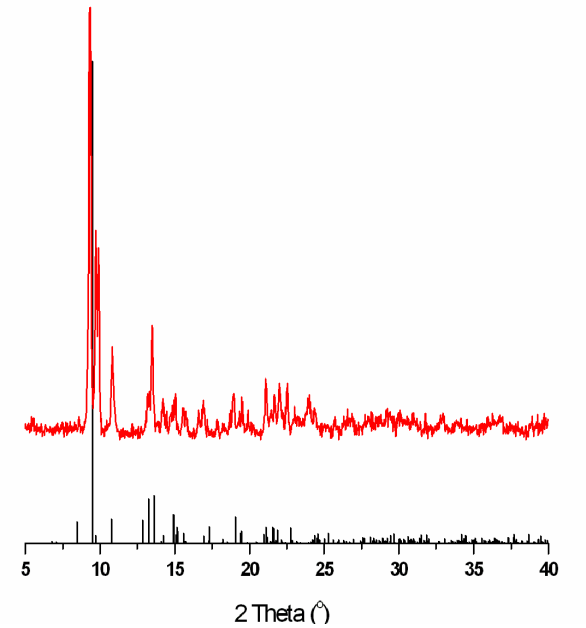

Figure S11. Top: XPRD patterns after re-cooking **1** in mixed H_2O/ethanol (1:3 ratio) solvent at 140 °C for 2 days; Bottom: calculated on the basis of the structure determined by single-crystal X-ray diffraction for **2**.